PROCEEDINGS OF SCIENCE

Recent Results from the FASTSUM Collaboration

Chris Allton,[a,*] Gert Aarts,[a,b] Ryan Bignell,[a] Tim Burns,[a] Sergio Chaves,[a] Simon Hands,[c] Benjamin Jäger,[d] Seyong Kim,[e] Maria Paola Lombardo,[f] Ben Page,[a] Sinéad M. Ryan,[g] Jon-Ivar Skullerud[h] and Thomas Spriggs[a] for the FASTSUM collaboration

[a] *Department of Physics, Swansea University, Swansea, SA2 8PP, United Kingdom*

[b] *European Centre for Theoretical Studies in Nuclear Physics and Related Areas (ECT*) Fondazione Bruno Kessler, Strada delle Tabarelle 286, 38123 Villazzano (TN), Italy*

[c] *Department of Mathematical Sciences, University of Liverpool, Liverpool L69 3BX, United Kingdom*

[d] *CP3-Origins & Danish IAS, Department of Mathematics and Computer Science, University of Southern Denmark, 5230, Odense M, Denmark*

[e] *Department of Physics, Sejong University, Seoul 143-747, Korea*

[f] *INFN, Sezione di Firenze, 50019 Sesto Fiorentino (FI), Italy*

[g] *School of Mathematics, Trinity College, Dublin, Ireland*

[h] *Department of Theoretical Physics, National University of Ireland Maynooth, County Kildare, Ireland*

E-mail: c.r.allton@swansea.ac.uk

The FASTSUM Collaboration has developed a comprehensive research programme in thermal QCD using 2 + 1 flavour, anisotropic ensembles. In this talk, we summarise some of our recent results including thermal hadron spectrum calculations using our "Generation 2L" ensembles which have pion masses of 239(1) MeV. These include open charm mesons and charm baryons. We also summarise our work using the Backus Gilbert approach to determining the spectral function of the NRQCD bottomonium system. Finally, we review our determination of the interquark potential in the same system, but using our "Generation 2" ensembles which have heavier pion masses of 384(4) MeV.

The 39th International Symposium on Lattice Field Theory (Lattice 2022),
8-13 August, 2022
Bonn, Germany

*Speaker

PoS(LATTICE2022)198

1. Introduction

The thermal spectrum of QCD is of great interest for intrinsic reasons in order to understand how confinement is manifest in hadronic systems. It is also crucial to aid the analysis of heavy-ion collision experiments. Here we present an update of the FASTSUM Collaboration's thermal hadronic spectrum research, focussing on open charm mesons, charm baryons and bottomonium. We also present an update of our studies of the interquark potential in bottomonium.

We use 2+1 flavour dynamical simulations with anisotropic latices where the temporal lattice spacing, a_τ, is smaller than the spatial one, a_s [1, 2]. Our anisotropy is designed to maximise information from thermal temporal correlators, noting that they are constrained in temporal extent, L_τ, since the temperature, $T = 1/L_\tau$. We use stout-linked, clover-improved Wilson fermions and Symanzik-improved gauge fields.

The lattice ensembles used in this work are our Generation 2 and 2L ensembles which have parameters listed in Tables 1 and 2. These ensembles have a pion mass of 384(4) and 239(1) MeV respectively and span temperatures both below and above the pseudocritical temperature $T_{\rm pc}$.

N_τ	128	40	36	32	28	24	20	16
T [MeV]	44	141	156	176	201	235	281	352

Table 1: Parameters for the FASTSUM Generation 2 ensembles used in this work. The lattice sizes are $24^3 \times N_\tau$, with lattice spacings $a_s = 0.1205(8)$ fm and $a_\tau = 35.1(2)$ am, and pion mass $m_\pi = 384(4)$ MeV. The vertical line indicates the position of $T_{\rm pc} \approx 181$ MeV. Full details in [1, 2].

N_τ	128	64	56	48	40	36	32	28	24	20	16
T [MeV]	47	95	109	127	152	169	190	217	253	304	380

Table 2: Parameters for the FASTSUM Generation 2L ensembles used in this work. The lattice sizes are $32^3 \times N_\tau$, with lattice spacings $a_s = 0.1121(3)$ fm and $a_\tau = 32.46(7)$ am, and pion mass $m_\pi = 239(1)$ MeV [3]. The vertical line indicates the position of $T_{\rm pc} \approx 167$ MeV. Full details in [2, 4].

2. Charm hadron spectrum

Here we summarise results from both open-charm mesons and charmed baryons using our Generation 2L ensembles.

Unlike hiddened-charmed mesons at non-zero temperature, which have been extensively studied on the lattice [5], open-charmed mesons have received less attention [6–8]. In [4], we present results for the open charm meson spectrum for $T \lesssim T_{pc}$. Because the states are confined, we proceed with conventional analysis techniques and assess up to which temperatures these are applicable. We extend these techniques to determine the variation of the masses as a function of temperature.

The results are shown in Fig.1. These show a small temperature variation where both the pseudoscalar, $D_{(s)}$, and vector, $D^*_{(s)}$, mesons' masses decrease as the temperature approches T_{pc}.

However, note that this temperature shift is at the percent level. In contrast, the analogous thermal effects for the axial vector and scalar channel are very strong, see [4] for details.

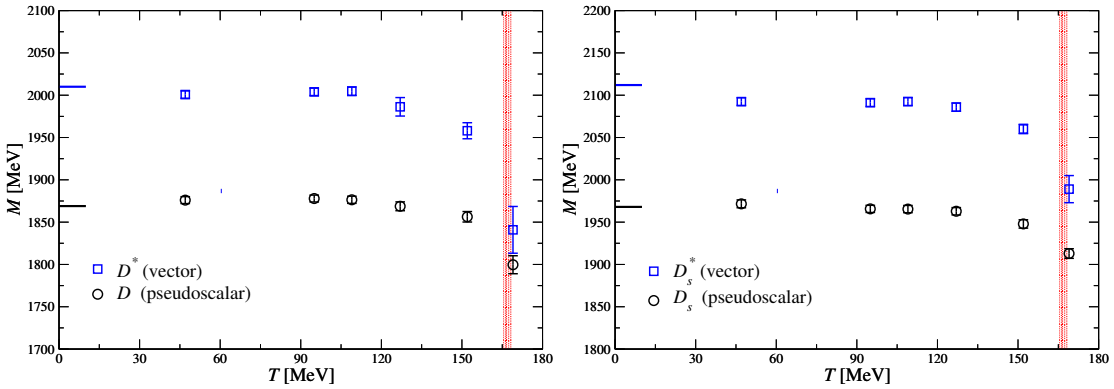

Figure 1: Temperature dependence of the groundstate masses in the hadronic phase, for D and D^* (left) and D_s and D_s^* (right) mesons. The vertical band indicates T_{pc} and the horizontal stubs at $T = 0$ represent the PDG values [9].

In another analysis [10, 11], we study the charm baryon spectrum paying particular attention to both parity states. We extract the masses in the confined phase and use a method based on a direct analysis of the correlation function to determine whether the parity states approach degeneracy for $T \geq T_{pc}$.

In Fig.2 we plot the masses for baryons with a variety of charm content as a function of T up to just beyond T_{pc} where the simple pole fits become unreliable.

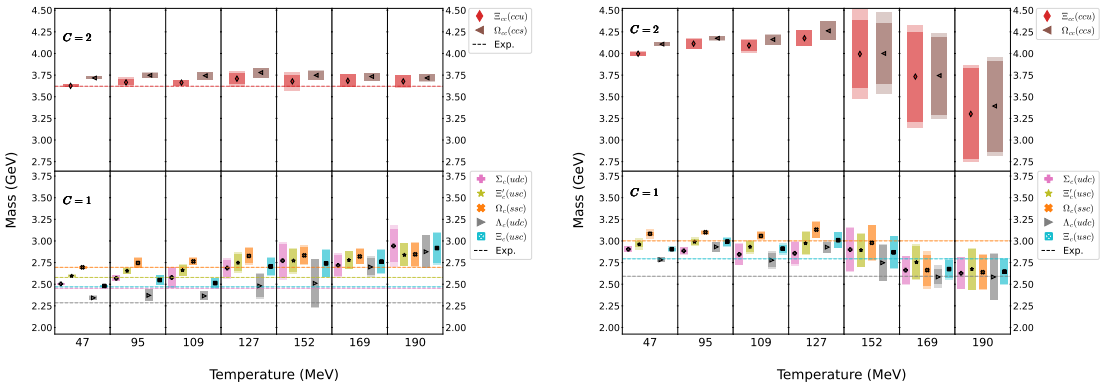

Figure 2: Mass spectrum of of the $J^{1/2+}$ baryons with positive (left) and negative parity (right) as a function of temperature. Dashed lines are zero-temperature experimental results [9] to guide the eye. The inner (outer) shaded regions represents the statistical (systematic) errors. See [10] for the corresponding plots for the $J^{3/2+}$ states.

For $T > T_{pc}$ we cannot assume that the charm baryon states are bound and so a conventional pole fitting ansatze cannot be applied. To gain information about the mass of the two parity states,

we therefore define the ratio R,

$$R(n_0) = \frac{\sum_{n=n_0}^{\frac{1}{2}N_\tau - 1} \mathcal{R}(\tau_n)/\sigma^2_{\mathcal{R}}(\tau_n)}{\sum_{n=n_0}^{\frac{1}{2}N_\tau - 1} 1/\sigma^2_{\mathcal{R}}(\tau_n)}, \qquad \text{where} \qquad \mathcal{R}(\tau) = \frac{G^+(\tau) - G^-(\tau)}{G^+(\tau) + G^-(\tau)}. \tag{1}$$

Typically we use $n_0 = 4$, and our results are not qualitatively sensitive to this choice. R will be unity in the limit of $M^+ \ll M^-$ and zero for the degenerate case. In Fig.3 we plot R for a number of channels. We can see an approach to degeneracy above T_{pc} which is most pronounced for baryons with the least charm content. By fitting the data to cubic splines, we can determine estimates of the transition temperatures from the inflection points and these are indicated as vertical lines in the figure. We note that the location of the inflection points coincide, within a few MeV, with the pseudocritical temperature, $T_{\rm pc} = 167(3)$ MeV, determined via the chiral condensate [4] and hence are a manifestion of chiral symmetry restoration in the charmed baryon sector. Further details about these points are elucidated in [10, 11].

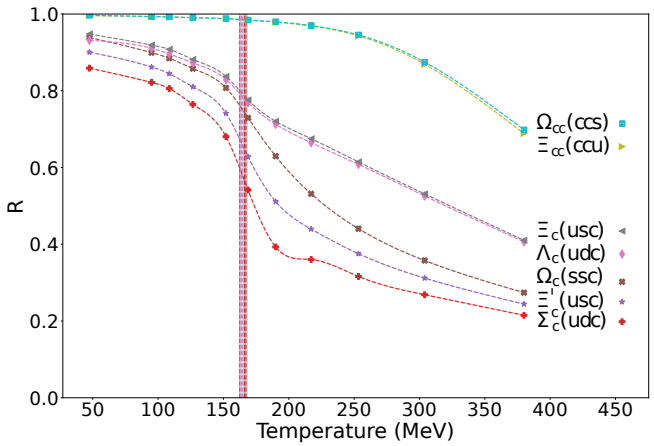

Figure 3: R value from Eq.(1) for $J = \frac{1}{2}$ baryons with the lines from cubic splines. The transition temperature estimates obtained from the inflection point of the splines are shown as vertical lines.

3. Bottomonium (NRQCD) spectrum

Bottomonium states are important probes of the quark gluon plasma phase in heavy-ion collision experiments because they are created very early and do not reach chemical equilibrium. The lattice approach to analysing bottomonium spectra invariably relies on extracting the spectral function at temperature T, $\rho(\omega, T)$, defined from the correlation function,

$$G(\tau; T) = \int_{\omega_{\rm min}}^{\infty} \frac{d\omega}{2\pi} K(\tau, \omega)\rho(\omega; T), \tag{2}$$

where the kernel for NRQCD quarks is defined as,

$$K(\tau, \omega) = e^{-\omega\tau}. \tag{3}$$

Note that since NRQCD introduces an additive energy shift, the lower limit of the integral in Eq.(2), ω_{min}, is not necessarily zero. The spectral function gives complete information about the spectrum of a particular channel, including the widths of the states. The FASTSUM Collaboration has studied the bottomonium spectrum using NRQCD bottom quarks in a number of publications, e.g. [12], using a variety of methods to extract the spectral function.

In [13] we extend this work by using the Backus Gilbert [14] method to obtain the spectral function with our Generation 2L ensembles, and we report on this work here. We note that we can introduce two "hyper-parameters" in our analysis. The first is the "whitening" factor, α, in the Tikhonov-like method [15], which governs how much of the identity (white noise) is added to the kernel. To remove the α dependency in the final result, the $\alpha \to 0$ limit is taken. The second parameter is an energy shift, Δ. Since Eq.(2) is a Laplace transform, we can trivially shift $\rho(\omega) \to \rho(\omega + \Delta)$ by multiplying $G(\tau)$ by $e^{\Delta\tau}$. Increasing the energy shift, Δ, moves the ground state feature closer to ω_{min} which is advantageous because that is where the Backus Gilbert method has the greatest resolution. Note however that the value of Δ needs to be limited to ensure that no spectral feature is pushed into the $\omega < \omega_{\mathrm{min}}$ region. Hence we remove the dependency on the Δ hyper-parameter via this requirement.

In Fig.4 we plot the χ_{b1} spectral function obtained from local correlators with various Δ values to illustrate that the ground state feature becomes better resolved as Δ increases. Full results and predictions of masses and widths obtained using this method are in [13].

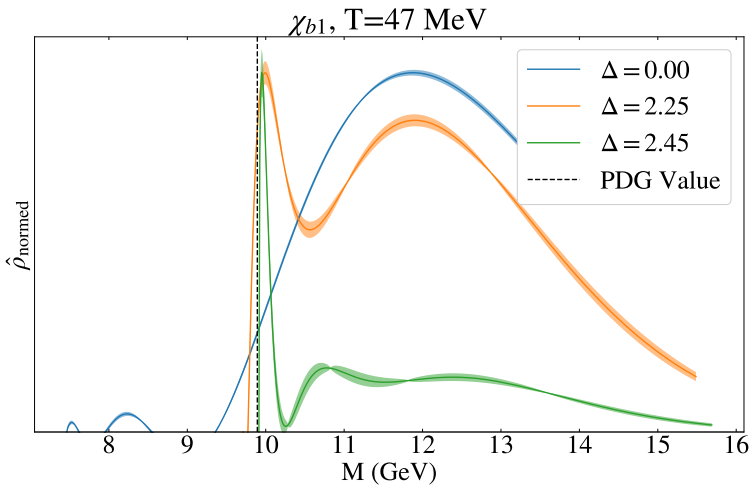

Figure 4: The χ_{b1} spectral function obtained via the Backus Gilbert method for a variety of Δ energy shifts at $T = 47$ MeV.

We can also perform an interesting statistical analysis of the correlation functions. As pointed out by Parisi and Lepage [16, 17], the statistical error of the hadronic correlation function, $\langle O(t)O(O)\rangle$ at large time is determined by the lightest states that can be composed from O^2. Typically this will be the pseudoscalar state.

We have analysed the statistical error in the bottomonium correlation functions by measuring their covariance matrices' singularity as the energy shift, $e^{\Delta\tau}$, is applied. The value of Δ corresponding to the most singular covariance matrix, Δ_{sing}, is a prediction of (half) the ground state

mass in the O^2 channel. We used the condition number of the covariance matrix to determine Δ_{sing}. Following the Parisi and Lepage analysis, we expect to find $\Delta_{\text{sing}} = M_{\eta_b}$ i.e. the mass of the pseudoscalar in the bottomonium sector.

In Fig.5 we plot results for the channels considered (η_b, Υ, h_b and $\chi_{\text{b0,b1,b2}}$) as a function of τ_2 where the covariance matrices are analysed over the time interval $[0, \tau_2/a_\tau]$. Smeared operators at both the source and sink were used. Figure 5 shows a convergence, as τ_2 increases, to a mass value compatible with the pseudoscalar, η_b, independent of the channel, as expected from an analysis following [16, 17]. Further details of this work are discussed in [13].

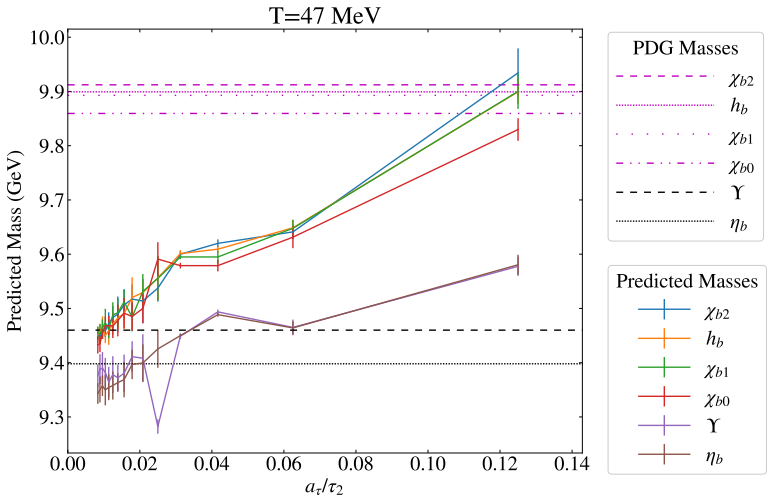

Figure 5: The value of the energy shift, Δ_{sing}, (i.e. the predicted mass) which gives the most singular covariance matrix for a variety of bottomonium channels as a function of $1/\tau_2$. The covariance matrices are defined over the time interval $[0, \tau_2/a_\tau]$ and therefore the best results are obtained as $\tau_2 \to \infty$. Experimental mass values are also shown as horizontal lines [9]. This indicates the method correctly predicts the η_b (i.e. the pseudoscalar) mass as τ_2 increases.

4. Interquark potentials in Bottomonium

For temperatures below T_{pc}, the interquark potential is known to be confining, i.e. with a non-zero string tension, whereas above T_{pc} it is expected to flatten allowing unbound quark states. Lattice studies of the interquark potential have been obtained from Wilson loops, which correspond to infinitely heavy quarks [18, 19], the NRQCD bottomonium system [20], and from charmonium using the HAL QCD method [21–23].

In this work, we study the interquark potential in the bottomonium system also using the HAL QCD approach, see [24]. The bottom quarks were simulated using the NRQCD approximation and our Generation 2 ensembles were used, see Table 1.

The HAL QCD method [25] uses Bethe Salpeter wavefunctions, $\psi(t, \vec{r})$, obtained from temporal correlators of non-local heavy quark–antiquark meson operators, $\overline{Q}(\tau, \vec{x})\Gamma Q(\tau, \vec{x} + \vec{r})$. It represents

the mesonic system with a Schrödinger equation,

$$\left[\frac{p^2}{2\mu} + V(\vec{r})\right]\psi(\tau,\vec{r}) = E\psi(\tau,\vec{r}), \tag{4}$$

where μ is the reduced quark mass in the centre of mass frame. The residual, non-physical $\tau-$dependency has to be carefully handled and this is discussed in [24].

Figure 6 shows the preliminary results for the interquark bottomonium potential for a variety of temperatures. In each pane, the *same* time window was considered, thus nullifying any systematic effects from this fitting artefact. These plots show evidence of the expected flattening of the potential as the temperature increases.

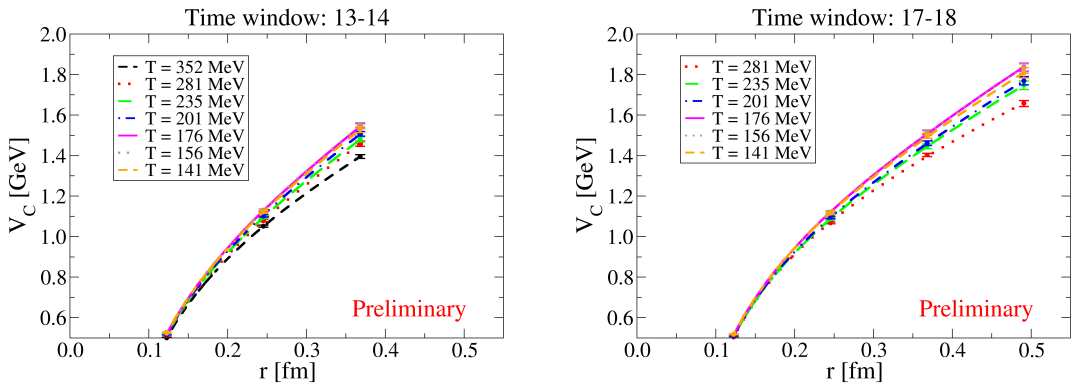

Figure 6: The interquark potential in (NRQCD) bottomonium via the HAL QCD procedure. In each pane, all the temperatures used the same time window: $[13, 14]$ (left) and $[17, 18]$ (right). This is to isolate thermal effects from τ systematics. The expected flattening of the potential with temperature can be seen.

5. Conclusions

Recent results from Fastsum Collaboration's thermal spectrum research [4, 10, 11, 13] and interquark potentials [24] have been presented.

6. Acknowledgements

This work is supported by STFC grant ST/T000813/1. SK is supported by the National Research Foundation of Korea under grant NRF-2021R1A2C1092701 and Grant NRF-2021K1A3A1A16096820, funded by the Korean government (MEST). BP has been supported by a Swansea University Research Excellence Scholarship (SURES). This work used the DiRAC Extreme Scaling service at the University of Edinburgh, operated by the Edinburgh Parallel Computing Centre and the DiRAC Data Intensive service operated by the University of Leicester IT Services on behalf of the STFC DiRAC HPC Facility (www.dirac.ac.uk). This equipment was funded by BEIS capital funding via

STFC capital grants ST/R00238X/1, ST/K000373/1 and ST/R002363/1 and STFC DiRAC Operations grants ST/R001006/1 and ST/R001014/1. DiRAC is part of the UK National e-Infrastructure. This work was performed using PRACE resources at Cineca (Italy), CEA (France) and Stuttgart (Germany) via grants 2015133079, 2018194714, 2019214714 and 2020214714. We acknowledge the support of the Swansea Academy for Advanced Computing, the Supercomputing Wales project, which is part-funded by the European Regional Development Fund (ERDF) via Welsh Government, and the University of Southern Denmark and ICHEC, Ireland for use of computing facilities. We are grateful to the Hadron Spectrum Collaboration for the use of their zero temperature ensemble in our Generation 2 work.

References

[1] G. Aarts, C. Allton, A. Amato, P. Giudice, S. Hands and J. I. Skullerud, JHEP **02** (2015), 186 [arXiv:1412.6411 [hep-lat]].

[2] G. Aarts, C. Allton, J. Glesaaen, S. Hands, B. Jäger, S. Kim, M. P. Lombardo, A. A. Nikolaev, S. M. Ryan and J. I. Skullerud, *et al.* Phys. Rev. D **105** (2022) no.3, 034504 [arXiv:2007.04188 [hep-lat]].

[3] D. J. Wilson, R. A. Briceno, J. J. Dudek, R. G. Edwards and C. E. Thomas, Phys. Rev. Lett. **123** (2019) no.4, 042002 [arXiv:1904.03188 [hep-lat]].

[4] G. Aarts, C. Allton, R. Bignell, T. J. Burns, S. C. García-Mascaraque, S. Hands, B. Jäger, S. Kim, S. M. Ryan and J. I. Skullerud, [arXiv:2209.14681 [hep-lat]].

[5] A. Rothkopf, Phys. Rept. **858** (2020), 1-117 [arXiv:1912.02253 [hep-ph]].

[6] A. Bazavov, F. Karsch, Y. Maezawa, S. Mukherjee and P. Petreczky, Phys. Rev. D **91** (2015) no.5, 054503 [arXiv:1411.3018 [hep-lat]].

[7] A. Kelly, A. Rothkopf and J. I. Skullerud, Phys. Rev. D **97** (2018) no.11, 114509 [arXiv:1802.00667 [hep-lat]].

[8] A. Bazavov, H. T. Ding, P. Hegde, O. Kaczmarek, F. Karsch, E. Laermann, Y. Maezawa, S. Mukherjee, H. Ohno and P. Petreczky, *et al.* Phys. Lett. B **737** (2014), 210-215 [arXiv:1404.4043 [hep-lat]].

[9] P. A. Zyla *et al.* [Particle Data Group], PTEP **2020** (2020) no.8, 083C01

[10] R. Bignell et al., PoS(**LATTICE2022**)170.

[11] G. Aarts et al., *in preparation*.

[12] G. Aarts, C. Allton, T. Harris, S. Kim, M. P. Lombardo, S. M. Ryan and J. I. Skullerud, JHEP **07** (2014), 097 [arXiv:1402.6210 [hep-lat]].

[13] B. Page et al., PoS(**LATTICE2022**)187.

[14] G. Backus, F. Gilbert, Geophys. J. R. Astron. Soc. 16 (1968) 169, DOI: 10.1111/j.1365-246X.1968.tb00216.x.

[15] A.N. Tikhonov, *On the Stability of Inverse Problems*, in *On the Stability of Inverse Problems*, vol.**39**, (USSR), pp. 195-198 (1943)

[16] G. Parisi, Phys. Rept. **103** (1984), 203-211

[17] G. P. Lepage, TASI Proceedings (1989) 97, CLNS-89-971.

[18] A. Bazavov *et al.* [HotQCD], Phys. Rev. D **90** (2014), 094503 [arXiv:1407.6387 [hep-lat]].

[19] Y. Burnier, O. Kaczmarek and A. Rothkopf, Phys. Rev. Lett. **114** (2015) no.8, 082001 [arXiv:1410.2546 [hep-lat]].

[20] R. Larsen, S. Meinel, S. Mukherjee and P. Petreczky, Phys. Rev. D **102** (2020), 114508 [arXiv:2008.00100 [hep-lat]].

[21] T. Kawanai and S. Sasaki, Phys. Rev. D **85** (2012), 091503 [arXiv:1110.0888 [hep-lat]].

[22] P. W. M. Evans, C. R. Allton and J. I. Skullerud, Phys. Rev. D **89** (2014), 071502 [arXiv:1303.5331 [hep-lat]].

[23] C. Allton, W. Evans, P. Giudice and J. I. Skullerud, [arXiv:1505.06616 [hep-lat]].

[24] T. Spriggs et al., PoS(**LATTICE2022**)192.

[25] S. Aoki *et al.* [HAL QCD], PTEP **2012** (2012), 01A105 [arXiv:1206.5088 [hep-lat]].